EARTHQUAKE ENGINEERING AND STRUCTURAL DYNAMICS
*Earthquake Engng Struct. Dyn.* 2000; **29**:241–257

# Control design for seismically excited buildings: sensor and actuator reliability

T. R. Alt[1], F. Jabbari[1,*] and J. N. Yang[2]

[1] *Department of Mechanical and Aerospace Engineering, University of California, Irvine, CA 92697, U.S.A.*
[2] *Department of Civil and Environmental Engineering, University of California, Irvine, CA 92697, U.S.A.*

SUMMARY

In this paper we present control design methods that provide desirable levels of performance and simultaneously account for actuator and sensor reliability (or malfunction) for buildings under seismic excitations. Performance is defined in terms of the disturbance attenuation (i.e. $L_2$ gain) from the disturbances to the controlled outputs of the system. The reliability of actuators and sensors refers to the deviation of actual control forces or actual sensor measurements from their ideal levels. Simulation results for a six-storey building are used to demonstrate the effectiveness of the control analysis and design method presented.


KEY WORDS: reliability; robust control; quadratic stability; linear matrix inequalities

## 1. INTRODUCTION

Intensive research efforts have been directed toward active control of civil infrastructure subject to strong wind gusts and earthquakes. Comprehensive literature in this subject can be found in Reference [1–3], etc. in which various techniques have been studied for the design of active controllers. These techniques include $\mu$-synthesis [4], neural network and fuzzy control [5], covariance control [6, 7], LQG or $H_2$ method [8], $H_\infty$ techniques [9–12], sliding mode control [13–17], polynomial control [18–20], etc. Full-scale implementations of active control systems on buildings and other structures have been made mainly for the response reduction due to strong winds e.g. [1, 3, 21–23, etc.], whereas full-scale active control systems against strong earthquakes are currently under investigation [e.g. Reference 3]. Recently, considerable emphasis and attention have been placed on benchmark problems by the international structural control community. A benchmark problem for active control of seismic-excited test models was presented in Reference [24] with participation from many international research groups to compare different

* Correspondence to: F. Jabbari, Department of Mechanical and Aerospace Engineering University of California, Irvine, CA 92697-3975, U.S.A.

Contract grant sponsor: NSF; contract grant number: CMS-96-15731.

CCC 0098–8847/2000/020241–17$17.50

*Received 22 April 1999*
*Accepted 25 August 1999*

control strategies [e.g. 25, 26]. More recently, a benchmark problem for wind excited 76-storey building and a second-generation benchmark problem for seismic-excited buildings have been presented [27, 28]. More recent efforts have been aimed at developing control techniques to address practical issues that arise in the implementation of full-scale control systems on structures.

For practical implementation of control systems, the issue of reliability of the actuators and sensors is of great concern. Often control hardware (e.g. actuator and/or sensor) is embedded in the structure and maybe hard to test and maintain. Also, the actuators are used very infrequently and function at large output levels only during severe earthquake episodes. As a result, during the earthquake episode feedback signals measured by sensors may deviate from the actual values whereas forces generated by the actuators may differ from the designed control force levels. This form of malfunction of the control system may result in a detrimental effect on the controlled structure. Consequently, a control design methodology that can incorporate the actuator and sensor reliability information is highly desirable.

In this paper, we consider control designs that guarantee desirable performance in the presence of potential control hardware malfunction. The framework used in the paper is deterministic and does not require statistical data. It also differs from traditional failure detection techniques in the sense that our controllers perform well in the face of sudden malfunction. Veillette *et al.* [29 and references therein], have examined the reliability of control systems for complete sensor and actuator outages. While the control techniques presented in this paper could perform this type of analysis and design, the approach used here is meant for systems where the actuator or sensor signals have gain deviations (or variations), particularly during the start-up period, but are not necessarily subject to complete failure. These variations could come from power fluctuations, non-linearities, partial actuator failure in parallel-type actuation or any type of variation that causes time varying gain changes in the sensor or actuator signals.

Owing to the inherent time variations in the actuator or sensor behaviour (e.g. during the start-up period), we rely on the quadratic stability approach to incorporate the reliability concerns discussed above. The analysis method can be used to evaluate the reliable performance of actuators and sensors for a given controller. This aids in identifying the critical hardware components (for service and maintenance schedule). Reliable performance implies that the system maintains a given level of disturbance attenuation in the presence of the modeled actuator and/or sensor uncertainties. The synthesis problem directly uses data on the hardware limitations to yield the best reliable performance possible, given the reliability (or malfunction) of the actuators and/or sensors. The analysis and state feedback synthesis problems are reduced to a finite-dimensional convex programming problem. Under some simplifying assumptions, the state feedback synthesis problem reduces to a single linear matrix inequality. This greatly reduces the numerical intensity and allows for systems with many actuators to be analysed. Solvability conditions are presented for the output feedback case. These conditions can be made convex under some simplifying assumptions and utilizing central controller gains.

Simulation results are presented for a six-storey full-scale building. The achievable disturbance attenuation level is computed for a wide range of actuator uncertainty. Significant improvement in the disturbance attenuation level is achieved in comparison with a nominal $H_\infty$ design, showing the benefit of incorporating the uncertainties into the design process. Simulation results demonstrate significant reduction in interstorey drifts due to an earthquake episode even in the presence of significant actuator variations.

 

## 2. MODEL FOR ACTUATOR AND SENSOR RELIABILITY

The basic approach for actuator and sensor reliability analysis is to include actuator and/or sensor uncertainties when analysing the performance of a system. Here, the actual control forces and actual sensor measurements are represented by

$$u_{i,\mathrm{actual}}(t) = [1 + \delta_{u_i}(t)]u_i(t) \quad \text{and} \quad y_{i,\mathrm{actual}}(t) = [1 + \delta_{y_i}(t)]\,y_i(t) \tag{1}$$

where $u_i(t)$, $i = 1, m$ and $y_i(t)$, $i = 1, l$ are the ideal control force (i.e. command input) and ideal sensor measurement, respectively. Variations in the control forces and sensor signals are represented by scalars $\delta_{u_i}$ and $\delta y_i$, respectively. A value of $\delta_{u_i} = 0.3$, for example, denotes that the $i$th actuator can vary from the ideal value within a 30 per cent band, and $\delta_{u_i} = -1$ indicates that the control design will take into account the possibility of complete failure of the $i$th actuator. Throughout this paper, we assume that $\delta_i(t) \geqslant -1$. This allows significant variation in the gain, but prevents the sign of the actual control input from becoming different from that of the command input. The issue of time delays (which can lead to a phase lag and thus different signs between actual and command inputs) can also be incorporated, as discussed in Section 5.1. A complete treatment of this issue, however, requires a great deal of details and is beyond the scope of this paper.

The representation used here is depicted by the block diagram in Figure 1. The uncertainties represent changes from the nominal actuator or sensor signals due to variations, which are not fixed in time. We can write the vector form of (1) as $u_{\mathrm{actual}}(t) = [I + \Delta_u(t)]u(t)$, where $\Delta_u(t)$ is a diagonal matrix which represents the actuator uncertainty.

Now, consider the building structure shown in Figure 2 and modelled by an $n$-degrees-of-freedom system

$$M\ddot{\bar{x}}(t) + C\dot{\bar{x}}(t) + K\bar{x}(t) = \bar{B}[I + \Delta_u(t)]u(t) + \bar{G}w(t) \tag{2}$$

where $\bar{x} \in \mathbb{R}^n$ is an $n$-vector denoting the deformation corresponding to each degree of freedom (i.e. interstorey drift). Matrices $M$, $K$, and $C$ are $n \times n$ mass, stiffness and damping matrices, respectively, and $w(t)$ is the disturbance vector representing the loading due to earthquake ground motion. The $m$-dimensional control vector $u(t)$ corresponds to the actuator forces (generated via active bracing systems (ABS) or an active mass damper (AMD) for example). The corresponding

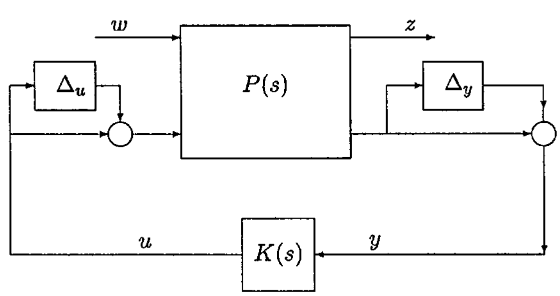


Figure 1. Actuator and sensor reliability framework.

 

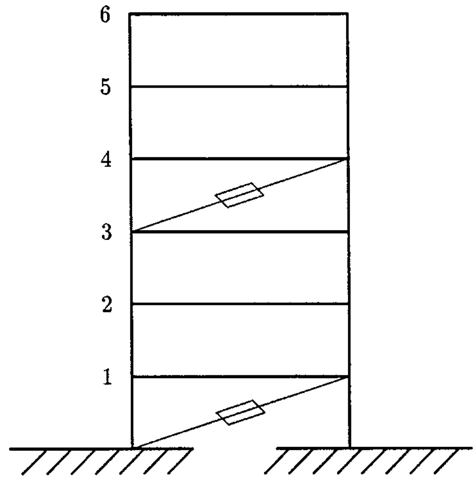


Figure 2. Schematic of building with active bracing system.

state space equations are given by

$$\begin{aligned}\dot{x}(t) &= Ax(t) + B_1 w(t) + B_2[I + \Delta_u(t)]u(t)\\ z(t) &= C_1 x(t) + D_{11} w(t) + D_{12}[I + \Delta_u(t)]u(t)\\ y(t) &= [I + \Delta_y(t)]C_2 x(t) + [I + \Delta_y(t)]D_{21} w(t)\end{aligned} \tag{3}$$

where $x(t) = [\bar{x}^{\mathrm{T}}(t)\ \dot{\bar{x}}^{\mathrm{T}}(t)]^{\mathrm{T}}$,

$$A = \begin{bmatrix} 0 & I \\ -M^{-1}K & -M^{-1}C \end{bmatrix},\quad B_1 = \begin{bmatrix} 0 \\ -M^{-1}\bar{G} \end{bmatrix},\quad B_2 = \begin{bmatrix} 0 \\ -M^{-1}\bar{B} \end{bmatrix}$$

and

$$\Delta_u(t) \in \underline{\Delta}_u = \{\mathrm{diag}\,[\delta_{u_1}, \delta_{u_2}, \ldots, \delta_{u_m}] : \delta_{u_i} \in [-\alpha_{u_i}, \alpha_{u_i}]\} \tag{4}$$

$$\Delta_y(t) \in \underline{\Delta}_y = \{\mathrm{diag}\,[\delta_{y_1}, \delta_{y_2}, \ldots, \delta_{y_l}] : \delta_{y_i} \in [-\alpha_{y_i}, \alpha_{y_i}]\} \tag{5}$$

or the combined form of

$$\Delta(t) = \mathrm{diag}\,[\Delta_u(t), \Delta_y(t)] \in \underline{\Delta} = \mathrm{diag}\,[\delta_{u_1}, \ldots, \delta_{u_m}, \delta_{y_1}, \ldots, \delta_{y_l}] \tag{6}$$

with the same bounds on the $\delta_{u_i}(t)$ and $\delta_{y_i}(t)$ as in Equations (4) and (5), respectively. These upper limits on the malfunction of the actuators and sensors, denoted by $\alpha_{u_i}$ and $\alpha_{y_i}$, are assumed to be known, but the actual variations (e.g. $\delta_{u_i}(t)$) are not known. The bounds are assumed to be symmetric (with respect to zero) to simplify the exposition. This does not cause any loss of generality, since non-symmetric bounds can be scaled by redefining the nominal $C_2$ and $B_2$ matrices. The actuator and sensor uncertainties, $\delta_{u_i}(t)$ and $\delta_{y_i}(t)$, are thus real and time varying,

 

but bounded, parameters. For future references we shall denote the vertex sets

$$\underline{\Delta}_{u_{\mathrm{vex}}} = \{\mathrm{diag}\,[\delta_{u_1}, \ldots, \delta_{u_m}] : \delta_{u_i} = \pm\, \alpha_{u_i}\} \tag{7}$$

$$\underline{\Delta}_{y_{\mathrm{vex}}} = \{\mathrm{diag}\,[\delta_{y_1}, \ldots, \delta_{y_l}] : \delta_{y_i} = \pm\, \alpha_{y_i}\} \tag{8}$$

$$\underline{\Delta}_{\mathrm{vex}} = \{\mathrm{diag}\,[\delta_{u_1}, \ldots, \delta_{u_m}, \delta_{y_1}, \ldots, \delta_{y_l}] : \delta_{u_i} = \pm\, \alpha_{u_i},\ \delta_{y_i} = \pm\, \alpha_{y_i}\} \tag{9}$$

It is easy to see that there are $2^{m+l}$ vertices for $\underline{\Delta}_{\mathrm{vex}}$. The basic control goal is to obtain a dynamic output feedback compensator of the form

$$\begin{aligned} \dot{x}_{\mathrm{c}}(t) &= A_{\mathrm{c}} x_{\mathrm{c}}(t) + B_{\mathrm{c}} y(t) \\ u(t) &= C_{\mathrm{c}} x_{\mathrm{c}}(t) + D_{\mathrm{c}} y(t) \end{aligned} \tag{10}$$

such that the closed-loop possesses desirable performance, for given bounds on the deviation of sensors and actuators from the ideal levels (i.e. for given $\alpha_{u_i}$ and/or $\alpha_{y_i}$). The resulting closed-loop system has the form

$$\dot{x}_{\mathrm{cl}}(t) = A_{\mathrm{cl}} x_{\mathrm{cl}}(t) + B_{\mathrm{cl}}(t) w(t) \tag{11}$$

where $x_{\mathrm{cl}}(t) = [x^{\mathrm{T}}(t)\ \ x_{\mathrm{c}}^{\mathrm{T}}(t)]^{\mathrm{T}}$, and $A_{\mathrm{cl}}$ and $B_{\mathrm{cl}}$ are

$$A_{\mathrm{cl}} = \begin{bmatrix} A + B_2(I + \Delta_u(t))D_{\mathrm{c}}(I + \Delta_y(t))C_2 & B_2(I + \Delta_u(t))C_{\mathrm{c}} \\ B_{\mathrm{c}}(I + \Delta_y(t))C_2 & A_{\mathrm{c}} \end{bmatrix} \tag{12}$$

$$B_{\mathrm{cl}} = \begin{bmatrix} B_1 + B_2(I + \Delta_u(t))D_{\mathrm{c}}(I + \Delta_y(t))D_{21} \\ B_{\mathrm{c}}(I + \Delta_y(t))D_{21} \end{bmatrix} w(t) \tag{13}$$

The controlled output is also simplified to

$$z(t) = C_{\mathrm{d}} x_{\mathrm{cl}}(t) + D_{\mathrm{cl}} w(t) \tag{14}$$

with

$$C_{\mathrm{cl}} = [C_1 + D_{12}(I + \Delta_u(t))D_{\mathrm{c}}(I + \Delta_y(t))C_2\ \ D_{12}(I + \Delta_u(t))C_{\mathrm{c}}] \tag{15}$$

and

$$D_{\mathrm{cl}} = D_{11} + D_{12}(I + \Delta_u(t))D_{\mathrm{c}}(I + \Delta_y(t))D_{21}$$

Note that the explicit dependence of $A_{\mathrm{cl}}$, $B_{\mathrm{cl}}$ and $C_{\mathrm{cl}}$ on $t$ (due to $\Delta_u(t)$ and $\Delta_y(t)$) is dropped to simplify the notations. We consider the resulting closed-loop system to have reliable performance if the controlled output, $z(t)$, satisfies the following equation in the presence of actuator and/or sensor uncertainties, assuming zero initial conditions

$$\int_0^\infty z^{\mathrm{T}}(t) z(t)\,\mathrm{d}t \leqslant \gamma^2 \int_0^\infty w^{\mathrm{T}}(t) w(t)\,\mathrm{d}t \tag{16}$$

which can also be written as $\|z(t)\|_2^2 \leqslant \gamma^2 \|w(t)\|_2^2$, where we have used the standard definition of the $L_2$ norm (energy) or a signal $\|z(t)\|_2^2 = \int_0^\infty z^{\mathrm{T}}(t)z(t)\,\mathrm{d}t$. As a result, $\gamma$ serves as the measure of performance and as it becomes small, the effects of the disturbance, $w(t)$, on $z(t)$ is diminished. For time-invariant systems, the notation in Equation (16) is interchangeable with having the infinity norm of the transfer function from $w$ to $z$, $T_{zw}$, be less than $\gamma$; i.e. $\|T_{zw}(s)\|_\infty \leqslant \gamma$ where the infinity norm is defined as $\|T_{zw}(s)\|_\infty = \sup_w \bar{\sigma}(T_{zw}(\mathrm{j}w))$ and $\bar{\sigma}$ denotes the maximum singular value. If Equation (16) holds, then we say the system has achieved disturbance attenuation of $\gamma$.

 

The closed loop has *reliable performance of* $\gamma$, if—for all allowable variations in the actuator and sensor behaviour—it satisfies Equation (16). Along the lines of Zhou *et al.* [30], this property holds if $R \triangleq \gamma^2 I - D_{11}^{\mathrm{T}} D_{11} > 0$ and there exists a positive definite $P$ such that

$$PA_{\mathrm{cl}} + A_{\mathrm{cl}}^{\mathrm{T}} P + \gamma^{-1} C_{\mathrm{cl}}^{\mathrm{T}} C_{\mathrm{cl}} + \gamma (PB_{\mathrm{cl}} + \gamma^{-1} C_{\mathrm{cl}}^{\mathrm{T}} D_u) R^{-1} (PB_{\mathrm{cl}} + \gamma^{-1} C_{\mathrm{cl}}^{\mathrm{T}} D_u)^{\mathrm{T}} < 0 \tag{17}$$

Equation (17) is referred to as an Algebraic Riccati inequality (ARI), in which the unknowns (e.g. $P$) appear non-linearity. Application of the Schur complement formula (see Reference [3]) to Equation (17) yields

$$\begin{bmatrix} PA_{\mathrm{cl}} + A_{\mathrm{cl}}^{\mathrm{T}} P & PB_{\mathrm{cl}} & C_{\mathrm{cl}}^{\mathrm{T}} \\ B_{\mathrm{cl}}^{\mathrm{T}} P & -\gamma I & D_u^{\mathrm{T}} \\ C_{\mathrm{cl}} & D_u & -\gamma I \end{bmatrix} < 0 \quad \text{for all } \Delta(t) \tag{18}$$

The goal is to design a controller such that Equation (18) holds for all values of $\Delta(t)$, which implied reliable performance of $\gamma$. In the next sections, it will be shown that the search for the controller matrices can be simplified and modified so that standard numerical algorithms can be used to obtain the desired controllers. We first study the state feedback case, in which the motivation for using a special structure for the dynamic output feedback controller becomes evident.

## 3. STATE FEEDBACK CONTROLLERS

In this section, we discuss the synthesis of the special case of full state feedback controllers for the actuator reliability problem. The motivations are (i) to simplify the overall exposition by establishing the results for a simpler case and then generalizing the results for the output feedback, and (ii) to highlight some of the special features of the state feedback problem (which are useful when the number of sensors is large enough so that system inversion techniques are possible—as discussed in Section 4).

Consider the system in (3) with $y(t) = x(t)$. The state feedback control problem consists of finding an appropriate control law of the form

$$u(t) = Kx(t) \tag{19}$$

such that the closed-loop system has reliable performance (with a desirable $\gamma$) for all allowable variations in the control (all allowable $\Delta_u(t)$). Using $u = Kx$, Equations (10)–(13) can be simplified. For example, Equation (19) is obtained by setting $A_{\mathrm{c}} = 0$, $B_{\mathrm{c}} = 0$, $C_{\mathrm{c}} = 0$, and $D_{\mathrm{c}} = K$. The availability of the states implies that $C_2 = I$, $D_{21} = 0$ and $\Delta_y(t) = 0$. Correspondingly, we have $A_{\mathrm{c}} = A + B_2(I + \Delta_u)K$, $B_{\mathrm{cl}} = B_1$, $C_{\mathrm{cl}} = C_1 + D_{12}(I + \Delta_u)K$ and $D_{\mathrm{cl}} = D_{11}$. The dimension of the inequality in Equation (17) is thus the same as that of $A$. Forming the bounded real inequality (i.e. Equation (18)), pre- and post-multiplying it with $P^{-1} = X$, one obtains the following form of Equation (18) for the state feedback problem

$$\begin{bmatrix} AX + XA^{\mathrm{T}} + B_2(I + \Delta_u)F + F^{\mathrm{T}}(I + \Delta_u)B_2^{\mathrm{T}} & B_1 & XC_1^{\mathrm{T}} + F^{\mathrm{T}}(I + \Delta_u)D_{12}^{\mathrm{T}} \\ B_1^{\mathrm{T}} & -\gamma I & D_{11}^{\mathrm{T}} \\ C_1 X + D_{12}(I + \Delta_u)F & D_{11} & -\gamma I \end{bmatrix} < 0 \tag{20}$$

The state feedback problem can now be stated as the following: There exists a state feedback controller such that the closed-loop system has reliable performance (of $\gamma$) if there exists matrices $F$ and $X > 0$ such that (20) holds *for all* $\Delta_u \in \underline{\Delta}_{u_{\text{vex}}}$, in which case the control low is given by $u(t) = FX^{-1}x(t)$.

In general, the inequality above needs to be satisfied for all values of $\Delta_u(t)$. Due to linearity, however, it suffices to have the inequality hold only at the vertices of the parameter set (see Reference [34] for details). As a result, Equation (20) represents a number of linear matrix inequalities (e.g. $2^m$), which are simultaneously satisfied with the same set of variables $(X, F)$. Finding $X$ and $F$ matrices such that the matrix inequalities (20) are satisfied constitutes a convex search, for which powerful techniques are available (see Reference [31, 32]). Consistent with control literature, throughout this paper, we refer to the searches in which unknown variables enter a set of linear matrix inequalities linearly as 'solving the LMIs'. As explained in Reference [31], the interior-point algorithms used in common software packages are guaranteed to find the solution (if one exists) with reasonable amount of computational burden.

The above result can be further simplified if

$$\text{(i) } D_{11} = 0, \quad \text{(ii) } D_{12}^{\mathrm{T}} C_1 = 0, \quad \text{(iii) } D_{12}^{\mathrm{T}} D_{12} > 0 \text{ and diagonal.} \tag{21}$$

The simplifying assumptions in Equation (21) correspond to the common case where there is no direct feed-through term from $w(t)$ to $z(t)$, and the dependence of the controlled output vector on the inputs and states can be decoupled (e.g. $z(t)$ consists of two variables appended into one vector, where the first is a function of the states and the second is a weighting on the controls). Finally, (iii) assumes that actuators are penalized independently. These assumptions are relatively common in many control system design methodologies, where dependence of $z(t)$ in $u(t)$ is strictly for manipulating the weighting on control. Under these simplifying assumptions, the inequality in Equation (20)—after applying standard Schur complement formula—becomes

$$AX + XA^{\mathrm{T}} + \gamma^{-1} X C_1^{\mathrm{T}} C_1 X + \gamma^{-1} B_1 B_1^{\mathrm{T}} + [\hat{B}_2 + F^{\mathrm{T}}(I + \Delta_u)] R_{\mathrm{c}} [\hat{B}_2 + F^{\mathrm{T}}(I + \Delta_u)]^{\mathrm{T}} - \hat{B}_2 R_{\mathrm{c}} \hat{B}_2^{\mathrm{T}} < 0 \tag{22}$$

where we have used $R_{\mathrm{c}} = \gamma^{-1} D_{12}^{\mathrm{T}} D_{12}$ and $\hat{B}_2 = B_2 R_{\mathrm{c}}^{-1}$. Selecting the structure of the so-called central feedback solution by imposing $F = -\hat{B}_2^{\mathrm{T}}$; i.e. $u(t) = -\hat{B}_2^{\mathrm{T}} X^{-1} x(t)$, we obtain the following:

$$AX + XA^{\mathrm{T}} + \gamma^{-1} X C_1^{\mathrm{T}} C_1 X + \gamma^{-1} B_1 B_1^{\mathrm{T}} - \hat{B}_2 (I - \Delta_u^2) R_{\mathrm{c}} \hat{B}_2^{\mathrm{T}} < 0, \ \forall \Delta_u \in \underline{\Delta}_u$$

which is true if and only if (see Reference [33] for details)

$$AX + XA^{\mathrm{T}} + \gamma^{-1} X C_1^{\mathrm{T}} C_1 X + \gamma^{-1} B_1 B_1^{\mathrm{T}} - \hat{B}_2 (I - \hat{\Delta}_u^2) R_{\mathrm{c}} \hat{B}_2^{\mathrm{T}} < 0$$

where $\hat{\Delta}_u = \operatorname{diag}[\alpha_{u_1}, \ldots, \alpha_{u_m}]$. Thus when the simplifying assumptions in Equation (21) hold, the central state feedback case reduces the number of LMIs from $2^m$ to only 1. In fact, a solution can be obtained by solving the algebraic Riccati equation (ARE) version of

$$AX + XA^{\mathrm{T}} + \gamma^{-1} X C_1^{\mathrm{T}} C_1 X + \gamma^{-1} B_1 B_1^{\mathrm{T}} - \hat{B}_2 (I - \hat{\Delta}_u^2) R_{\mathrm{c}} \hat{B}_2^{\mathrm{T}} + \varepsilon I = 0$$

whose solution will satisfy the inequality and greatly reduces the computational requirements for systems with many actuators. Note that in all cases (with or without simplifying assumptions), there exists a tradeoff between large $\Delta_u(t)$ (more severe deviation) and lower $\gamma$ (better performance). This

 

allows the achievable disturbance attenuation level to be computed as a function of actuator uncertainty, as will be demonstrated in Section 5 below.

For the state feedback case, the choice of the special controller (i.e. $F = -\hat{B}_2^{\mathrm{T}}$) primarily reduces the computational burden associated with the controller design, since the more general form is still a convex problem. The conservatism due to this form appears to be rather modest (see Reference [33]). In the case of output feedback, however, such a structure becomes critical in rendering the problem convex, since the general output feedback problem does not result in a convex search problem.

## 4. OUTPUT FEEDBACK

In this section we discuss the synthesis of output feedback controllers for the actuator and sensor reliability problem. In most problems, a strictly proper controller (i.e. $D_{\mathrm{c}} = 0$) is used due to the fact that a direct feed-through from the sensors may lead to undesirable levels of noise in the control. Furthermore, in many applications, the use of a strictly proper control does not result in any loss of generality [25, 34]. As a result, in the design of output feedback control laws, we only consider the strictly proper controllers, which also simplifies the exposition a great deal.

Thus, the problem is finding a controller as in Equation (10)—with $D_{\mathrm{c}} = 0$, such that inequality in Equation (18) holds for all allowable $\alpha_i$. Following the approach used in Reference [33, 35]—which includes a variety of change-of-co-ordinates and other linear algebra techniques, it can be shown that there exists an output feedback controller (as in Equation (10)) such that the closed-loop system has reliable performance of $\gamma$ (i.e. Equation (18) holds for the closed loop) if there exists matrices $X > 0$, $Y > 0$, $F$, $G$, and $L$ such that

$$\begin{bmatrix} \Psi_{11} & \Psi_{12} \\ \Psi_{21} & \Psi_{22} \end{bmatrix} < 0 \quad \forall \Delta(t) \tag{23}$$

and

$$\begin{bmatrix} X & I \\ I & Y \end{bmatrix} > 0 \tag{24}$$

where

$$\Psi_{11} = \begin{bmatrix} AX + XA^{\mathrm{T}} + B_2(I + \Delta_u(t))F + F^{\mathrm{T}}(I + \Delta_u(t))B_2^{\mathrm{T}} & A + L^{\mathrm{T}} + F^{\mathrm{T}}\Delta_u(t)B_2^{\mathrm{T}}Y + XC_2^{\mathrm{T}}\Delta_y(t)G^{\mathrm{T}} \\ A^{\mathrm{T}} + L + YB_2\Delta_u(t)F + G\Delta_y(t)C_2X & YA + A^{\mathrm{T}}Y + G(I + \Delta_y(t))C_2 + C_2^{\mathrm{T}}(I + \Delta_y(t))G^{\mathrm{T}} \end{bmatrix} \tag{25}$$

$$\Psi_{12} = \begin{bmatrix} B_1 & XC_1^{\mathrm{T}} + F^{\mathrm{T}}(I + \Delta_u(t))D_{12}^{\mathrm{T}} \\ YB_1 + G(I + \Delta_y(t))D_{21} & C_1^{\mathrm{T}} \end{bmatrix} \tag{26}$$

$$\Psi_{22} = \begin{bmatrix} -\gamma I & D_{11}^{\mathrm{T}} \\ D_{11} & -\gamma I \end{bmatrix}. \tag{27}$$

Once, $L$, $Y$, $X$, $F$ and $G$ are found such that Equation (23) and (24) are satisfied, one set of controller matrices that yield the desired reliable performance is obtained from the

 

following (see Reference [33, 34]):

$$\begin{aligned} A_c &= (Y - X^{-1})^{-1}(YAX + YB_2F + GC_2X - L)X^{-1} \\ B_c &= -(Y - X^{-1})^{-1}G \\ C_c &= FX^{-1} \end{aligned} \tag{28}$$

Due to the terms that include both $F$ and $Y$ (or $X$ and $G$) in Equation (25), the search for the matrices $X$, $Y$, etc. is bi-linear and, thus, not convex. As a result, the problem of obtaining a general output feedback controller is not easily solved. One approach is based on a two-step procedure in which the state feedback problem is solved in the first step. This first step, as discussed earlier, constitute a convex search and is easy to find the appropriate $X$ and $F$ matrices. In the second step, an observer-based controller is designed by finding an observer that combined with the state feedback gain, obtained in the first step, satisfies Equation (18). In this second step, since $X$ and $F$ are already known, the remaining parameters appear linearly in Equation (23), and thus the search for the observer parameters is convex. In general, such a technique is not guaranteed to yield a desirable controller, in the sense that the search in the second step may not be feasible. However, if the number and location of the sensors are chosen properly, the success of such a procedure can be guaranteed (see Reference [33, 35] for relevant details).

Another approach, which is well suited for the reliability problem studied here, is to rely on the specific structure of the central controller discussed earlier in the state feedback result. For this, let us assume that the simplifying assumptions of the previous section (i.e. Equation (21)) still holds and, in addition, we have

$$B_1D_{21}^{\mathrm{T}} = 0, \quad D_{21}D_{21}^{\mathrm{T}} > 0 \tag{29}$$

Then, using the following structure—which is the generalization of central controller in the state feedback problem –

$$F = -\gamma(D_{12}^{\mathrm{T}}D_{12})^{-1}B_2^{\mathrm{T}}, \quad G = -\gamma C_2^{\mathrm{T}}(D_{21}D_{21}^{\mathrm{T}})^{-1} \tag{30}$$

we can eliminate the bi-linear terms in Equation (26) and yield a set of matrix inequalities in which the remaining variables ($X$, $Y$, and $L$) appear linearly. Also, similar to the state feedback case, due to the linearity of matrix inequalities, the inequalities need to hold only at the vertices. Consequently, the design of output feedback controllers becomes a convex search.

*Remark* 1. The result presented so far are concerned with the synthesis problem. The framework used here can easily be applied as an *analysis* tool in reliability study for other control techniques. For example, a controller based on pole placement or $H_2$ techniques can be evaluated for its disturbance attenuation and reliability characteristics, through the use of Equation (18). In such a case, since the controller is known, Equation (18) can be used either to find the optimal $\gamma$ for given bounds on the actuator variations or to find the maximum allowable size of $\delta_{u_i}$ for a desired performance. Also note that both pole placement and $H_2$ problems have their own linear matrix inequality representation and can be used in the preceding results in stead of the $L_2$ gain approach presented (for synthesis).

*Remark* 2. As mentioned earlier, there is a natural trade-off between larger levels of variations allowed vs. performance. The technique presented here can be used (via a routine search) to obtain such tradeoff for each actuator and/or sensor. Such information can be used for hardware specification or identification of critical hardware for stringent maintenance and testing.

 

## 5. APPLICATION TO SIX-STOREY BUILDING

We consider a shear-beam model for a full-scale six-storey building with identical storey units. There are two actuators, one in the first storey unit and another in the third storey unit, both active bracing systems, as shown in Figure 2. The model is similar to the one used in References [9, 10]. The mass of each floor, and the stiffness and damping coefficients of each storey unit are $m_i = 345.6$ metric ton, $k_i = 340, 400$ kN/m, and $c_i = 2{,}937$ kN s/m, respectively. These values result in a first vibrational mode of 1.2 Hz, with a damping ratio of approximately 3.2 per cent. The total building weight, which is used later for comparison with peak actuator force, is 20,342 kN. Using $\bar{x}(t)$ as the vector of the interstorey drifts and $w(t)$ as the earthquake ground acceleration, a straight forward manipulation results in the following for Equation (2):

$$M^{-1}K = \frac{k_i}{m_i}\begin{bmatrix} 1 & -1 & 0 & 0 & 0 & 0 \\ -1 & 2 & -1 & 0 & 0 & 0 \\ 0 & -1 & 2 & -1 & 0 & 0 \\ 0 & 0 & -1 & 2 & -1 & 0 \\ 0 & 0 & 0 & -1 & 2 & -1 \\ 0 & 0 & 0 & 0 & -1 & 2 \end{bmatrix}, \quad M^{-1}\bar{B} = \frac{1}{m_i}\begin{bmatrix} 1 & 0 \\ -1 & 0 \\ 0 & 1 \\ 0 & -2 \\ 0 & 1 \\ 0 & 0 \end{bmatrix},$$

$$M^{-1}\bar{G} = \frac{1}{m_i}\begin{bmatrix} -1 \\ 0 \\ 0 \\ 0 \\ 0 \\ 0 \end{bmatrix}$$

and $M^{-1}C$ with the same form as $M^{-1}K$ (with $c_i$ instead of $k_i$). For the controlled output, we use

$$z(t) = \begin{bmatrix} H \\ 0 \end{bmatrix} x(t) + \begin{bmatrix} 0 \\ R_u \end{bmatrix} [I + \Delta_u(t)]\, u(t) \tag{31}$$

where $H$ is a $r \times 12$ matrix and $R_u$ is a $2 \times 2$ diagonal matrix. This form satisfies the simplifying assumptions in Equation (29). The weighted control is included in the $z$-vector to allow penalizing large control input forces. By decreasing $R_u$ we diminish the weighting on the control and place more emphasis on the states. For the results presented here, we select $H$ such that it places equal weights for all interstorey drifts; i.e. $H = [I_6 \; 0_6]$, where $I_6$ is a $6 \times 6$ identity matrix and $0_6$ is a $6 \times 6$ zero matrix. Naturally, further iterations can be used to fine tune and to improve the overall performance of the control system.

We start with the state feedback design, which was presented in Section 3. The control weighting matrix, $R_u$, was $R_u = \text{diagonal}\,(2.5 \times 10^{-6}, 2.5 \times 10^{-6})$. The best achievable disturbance attenuation level was computed for different cases in which the bounds on the actuator uncertainties (i.e. $\alpha_{u_i}$) was varied from 0 to 90 per cent. The results are presented in Figure 3. For simplicity, the same level of

 

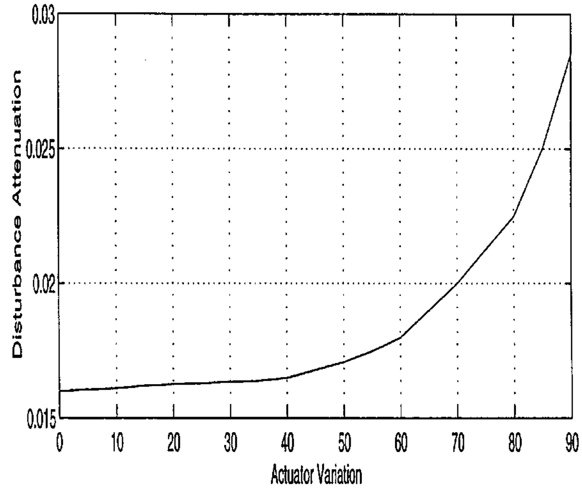


Figure 3. Performance level $\gamma$ in the presence of actuator variation $\alpha_u$.

malfunction is used for both actuators and it is assumed that the behaviour is symmetric with respect to the nominal value (both can be modified to include more general cases easily). As a result, $\alpha = 0.3$ denotes the case in which each actuator is assumed to behave only within 30 per cent of the ideal behaviour, or $-0.3 \leqslant \delta_u(t) \leqslant 0.3$. As expected, as the level of potential variation is increased (i.e., larger $\alpha_{u_i}$), the performance guarantee worsens (i.e. larger $\gamma$). The open-loop disturbance attenuation level $\gamma$ is 0.1475, indicating that we were able to significantly improve the disturbance attenuation in the presence of large variations of actuators. For example, variation levels of 0.5 (i.e. 50 per cent different from nominal) result in guaranteed performance levels that are approximately 40 per cent worse than the nominal or ideal performance.

To study the benefits of including the actuator variation model in the design process, the following comparison was made. First, a nominal $H_\infty$ controller was obtained assuming no actuator variations. Keeping this compensator fixed, (18) was used to obtain the effective disturbance attenuation of the *nominal* closed loop (i.e. with nominal controller) for given actuator/sensor variations levels. For each level of variation (i.e. $\alpha_u$), this is accomplished by finding positive definite $P$ while minimizing $\gamma$. Next, we obtain reliable compensators by using the procedures in Section 3; i.e. for each $\alpha_u$, we search for $X$ and $F$ that yield the best $\gamma$ (e.g. via Equation (20)). Figure 4 shows the improvement in the disturbance attenuation level $\gamma$ by incorporating actuator uncertainties in the design process. As observed from Figure 4, significant improvement has been achieved, particularly at the higher ranges of actuator uncertainties, as compared to the nominal $H_\infty$ design.

Next, we study the design output feedback controller for the case where the whole state vector is not available for measurement. For the results shown here, we have selected three (relative to ground) velocity sensors placed on the first-, third- and fifth-storey units. Similar results are obtained when either accelerations or relative displacements (drifts) are measured. The measured output is then

$$y(t) = C_2 x(t) + D_{21} \hat{w}(t)$$

 

Table I. Performance $\gamma$ vs. actuator variation level $\alpha_u$.

| Actuator variation level $\alpha_u$ | State feedback attenuation $\gamma$ | Output feedback attenuation $\gamma$ |
|---|---|---|
| 0.0 | 0.0162 | 0.0162 |
| 0.1 | 0.0163 | 0.0164 |
| 0.2 | 0.0164 | 0.0168 |
| 0.3 | 0.0167 | 0.0177 |
| 0.4 | 0.0171 | 0.0193 |
| 0.5 | 0.0177 | 0.0228 |
| 0.6 | 0.0186 | 0.0253 |
| 0.7 | 0.0212 | 0.0281 |
| 0.8 | 0.0229 | 0.0356 |

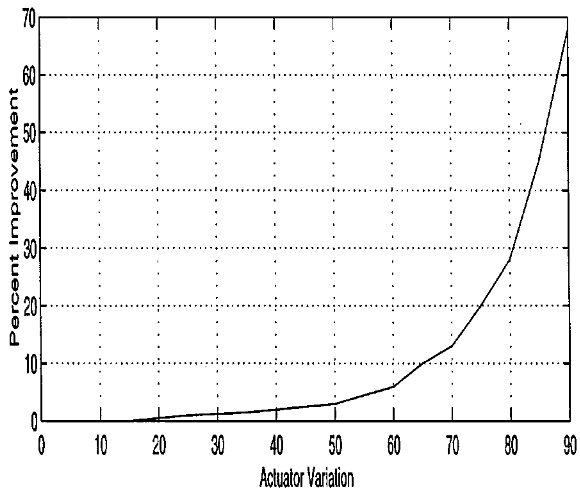


Figure 4. Performance improvement (i.e. $\gamma$) over nominal design vs. actuator variation $\alpha_u$.

where $\hat{w}(t) = [w^{\mathrm{T}}(t)\, n^{\mathrm{T}}(t)]^{\mathrm{T}}$ and $n(t)$ is sensor noise. We also use $D_{21} = [0, R_y]$, where $R_y = 10^{-3} I_3$ is the weighting on the sensor noise. Matrix $C_2$ is a $3 \times 12$ matrix that corresponds to the relative velocities of first, third and fifth floors from the ground.

An $H_\infty$ output feedback design was generated for the nominal system. Due to the relatively large number of sensors and low sensor noise, the disturbance attenuation for the output feedback controller was 0.016201 (virtually the same as that of the state feedback controller). For brevity, we only consider variations in the actuators. Reliable output feedback designs that minimize the disturbance attenuation level $\gamma$ were generated for various actuator variation ranges from 0 to 90 per cent using conditions in Equations (23) and (24). Since we did not model any sensor variation, it was not necessary to use the central control gain for $G$, and $G$ was left as an unknown variable in the search. A bisection method was used to find the lowest disturbance attenuation level ($\gamma$) such that

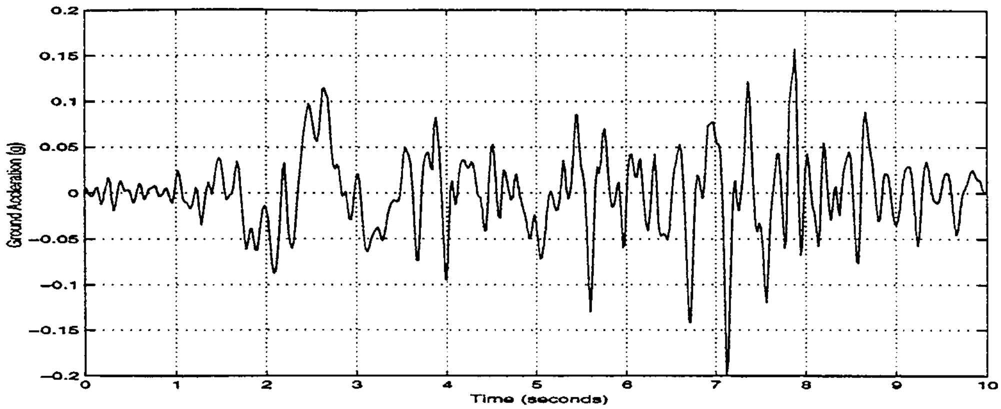


Figure 5. Ground acceleration record (0.2 g PGA).

Table II. Peak response quantities for different levels of actuator variations using $\alpha_u = 0.3$.

| Case | A | B | C | D | E | F |
|---|---|---|---|---|---|---|
| $\delta_{u1}$ | N/A | − 0.3 | − 0.2 | 0.3 | − 0.3 | − 0.2 |
| $\delta_{u2}$ | N/A | − 0.3 | − 0.2 | 0.3 | 0.1 | 0.1 |
| $u_{1_{\max}}$ (kN) | 0 | 1916 | 1782 | 1472 | 1777 | 1688 |
| $u_{2_{\max}}$ (kN) | 0 | 1338 | 1246 | 994 | 1235 | 1177 |
| $x_1$ (cm) | 1.06 | 0.63 | 0.60 | 0.50 | 0.60 | 0.58 |
| $x_2$ (cm) | 0.95 | 0.71 | 0.70 | 0.65 | 0.69 | 0.68 |
| $x_3$ (cm) | 0.81 | 0.59 | 0.58 | 0.53 | 0.57 | 0.56 |
| $x_4$ (cm) | 0.65 | 0.38 | 0.37 | 0.34 | 0.41 | 0.39 |
| $x_5$ (cm) | 0.47 | 0.31 | 0.30 | 0.27 | 0.29 | 0.29 |
| $x_6$ (cm) | 0.25 | 0.16 | 0.16 | 0.14 | 0.15 | 0.15 |

there exists matrices that satisfy Equations (23) and (24). The resulting disturbance attenuation levels are summarized in Table I along with the state feedback design results. Note that the state feedback designs are optimal because they used both necessary and sufficient conditions (see Reference [33] for details), while the output feedback may be sub-optimal because they are constrained to using the central controller gain for $F$. The output feedback attenuation levels are quite similar to those of the state feedback for low levels of actuator variations. As the size of the modelled variation increases, however, the conservatism—due to the use of the special structure for $F$—may grow. It should be noted that the optimal $H_\infty$ output feedback controller for the nominal system becomes unstable when analysed for actuator variations greater than 10 per cent.

To evaluate the performance of these reliable controllers in reducing the interstorey drifts, the Pacoima earthquake ground motion record, scaled to a peak ground acceleration of 0.2 g as shown in Figure 5, was used to obtain the response time histories of the closed-loop system. Peak response quantities of time histories are shown in Table II, in which $x_i$ (in cm) is the peak interstorey drift of the $i$th storey unit and $u_{i_{\max}}$ denotes the peak control force for the $i$th actuator. Since the model is linear, the structures response to a stronger or weaker ground motion can be obtained by a simple

 

Table III. Reliability with respect to time delays and malfunction.

| Perturbation | Delay (s) | Peak drifts in per cent improvement from open loop | | | | | | Per cent building weight | |
|---|---|---|---|---|---|---|---|---|---|
| | | $x_1$ | $x_2$ | $x_3$ | $x_4$ | $x_5$ | $x_6$ | $u_1$ | $u_2$ |
| None | 0 | 47.9 | 29.0 | 30.8 | 45.7 | 38.9 | 39.1 | 7.76 | 5.38 |
| Average | 0 | 47.6 | 28.8 | 30.7 | 44.3 | 38.1 | 38.6 | 7.95 | 5.50 |
| Worst case | 0 | 40.8 | 24.9 | 26.6 | 31.4 | 32.8 | 32.5 | 9.42 | 6.58 |
| None | 0.02 | 55.4 | 26.7 | 30.1 | 50.0 | 31.5 | 22.4 | 8.85 | 6.05 |
| Average | 0.02 | 54.7 | 26.6 | 30.0 | 47.5 | 30.5 | 22.3 | 8.90 | 6.12 |
| Worst case | 0.02 | 47.8 | 23.8 | 26.9 | 33.1 | 23.1 | 15.2 | 11.52 | 8.36 |

scaling. The most intense portion of the earthquake occurred during the first 10 s, Figure 5 and the simulated peak responses reported below concern this period.

Table II shows the results for representative variation levels, in which all data correspond to a single control law. This control law was designed to tolerate a 30 per cent malfunction in each actuator (i.e. an $\alpha_u$ of 0.3 was used for the controller design). With such a controller, simulations results were obtained by assuming different actual malfunction levels of actuators, as denoted by $\delta_{u_1}$ and $\delta_{u_2}$ in Table II. Case A is the open-loop response of the structure to the (0.2 g peak acceleration) ground motion. Different columns of Table II correspond to the controller performance for different actual malfunction levels $\delta_{u_i}$ (which are unlikely to be exactly 30 per cent during operation). For example, Case C presents the results in which both actuators perform at 80 per cent of the nominal level; i.e. $\delta_{u_1} = \delta_{u_2} = -0.2$. As Table II indicates, our technique is successful in obtaining good performance levels, even in the presence of significant hardware malfunction. The values listed for the peak control force are the ideal (command) levels. Actual force levels are the nominal ones times $(1 + \delta_{u_i})$. Note that the actual forces (or the ideal ones) are always less than 10 per cent of the building weight.

Next, the time histories of the response quantities, with the same controller that was used for Table II, have been computed for the open-loop system and 48 cases of the closed-loop system. The actuator deviations $\delta_{u_1}$ and $\delta_{u_2}$ (which were set to be constants for ease of simulation) corresponded to a 10 per cent grid of the uncertainty parameter space (i.e. $\delta_{u_1}$ and $\delta_{u_2}$ having any combinations of values $-0.3$, $-0.2$, $-0.1$, 0.0, 0.1, 0.2 and 0.3). The peak response quantities, $x_i$, and control forces, $u_i$, are summarized in Table III. In the first row of Table III, 'None' denotes the case where no actuator deviation was used. In the second and third rows, denoted by 'average' and 'worst', respectively, the peak response quantities correspond to those cases (among 49 simulations) where the closed-loop behaviours were in the mid-range and the worst of the performances of the total 49 simulations. The peak drifts are typically reduced by 30–50 per cent of the corresponding values for the open-loop case. Since the total building weight is approximately 20,342 kN, the maximum actual control forces are less than 10 per cent of the total weight.

### 5.1. *Effects of small time delays*

The approach used in this paper for the actuator (or sensor) variations allows significant error in gain, but requires the actual control forces and command signals to have the same sign. In some

applications, significant time delays may lead to phase variations and error in the sign (as well as the magnitude). Due to the robustness of the quadratic stability technique used here, the closed-loop system can tolerate certain amount of time delays. If the delays are substantial, the basic framework used here can be extended to address this issue. While a detailed treatment is beyond the scope of this paper, we *briefly* discuss two mechanism for time delays and their effects on the performance.

In most applications, the control system will be implemented on a digital computer. This requires the analog control design to be converted to a discrete control system. The zero-order hold effect of the discretization along with the computational delay will add phase lag to the system. To study these effects, simulation results were generated for the discretized controller. The discrete time controller is given by

$$x_c(k) = A_c^d x_c(k-1) + B_c^d y(k-1)$$
$$u(k) = C_c x_c(k) + D_c y(k)$$

where $A_c^d = \exp(A_c \tau)$, $B_c^d = A_c^{-1}[\exp(A_c \tau) - I]B_c$ and $\tau$ is the sampling time. We assumed a sample time of 0.02 s or a 50 Hz sampling rate, which is only 5 times the highest-frequency mode in the model. A full cycle delay was also included in the simulation results. Simulation results by introducing time delays are summarized in the last three rows of Table III. Comparing these results to those with no time delay (the first three rows of Table I) indicates that, for small delays, the discretization and delay effects caused only a slight degradation in the closed-loop performance.

When the delays are substantial, the issue of time delay could also be formally considered from a continuous time perspective using the results in Reference [36]. A delay in the actuation of control commands results in the following differential delay equation:

$$\begin{bmatrix} \dot{x}(t) \\ \dot{x}_c(t) \end{bmatrix} = \begin{bmatrix} A & 0 \\ B_c(I + \Delta_y(t))C_2 & A_c \end{bmatrix} \begin{bmatrix} x(t) \\ x_c(t) \end{bmatrix} + \begin{bmatrix} 0 & B_2(I + \Delta_u(t))C_c \\ 0 & 0 \end{bmatrix} \begin{bmatrix} x(t-\tau) \\ x_c(t-\tau) \end{bmatrix}$$

which can be represented by

$$\dot{x}_{cl}(t) = [A_n + \Delta_{A_n}(t)]x_{cl}(t) + [A_{cl} + \Delta_{A_d}(t)]x_{cl}(t-\tau)$$

with obvious notations for $A_n$ and $A_d$. Following the development in Reference [36], the uncertainties (which are due to actuator and sensor malfunctions and variations) are modelled as norm bounded structured uncertainty and sufficient conditions can be obtained which, when satisfied, guarantee stability of the delayed system. The conditions in Reference [36] were 'delay dependent', i.e. the delay explicitly enters in the equations. As a result, this approach can be used to find the (smallest or critical) value of the delay that might lead to instability. Extension of the results of [36] for guaranteed performance and output feedback synthesis is possible but it is beyond the scope of this paper.

## 6. CONCLUSIONS

In this paper we presented a method for the analysis and design of controlled systems to achieve reliable performance. Reliable performance implies that the system maintains a given level of disturbance attenuation ($L_2$ or energy gain) in the presence of actuator and sensor uncertainties (or malfunction). The analysis case reduced to solving a set of LMIs for which efficient computational

 

algorithms have been developed. The synthesis of state feedback controllers reduced to solving a single LMI, where a solution could also be obtained by solving an algebraic Riccati equation. This greatly reduces the numerical intensity and allows state feedback controllers to be easily designed for systems with many actuators. Solvability conditions were presented for the output feedback case. By utilizing the central controller gains these conditions become LMIs which are easily solved. Results were presented for a six-storey building to illustrate the effectiveness of the control analysis and design methods presented.

## ACKNOWLEDGEMENTS

This research was supported by NSF grant CMS-96-15731.

## REFERENCES

1. Spencer BF, Sain MK. Controlling buildings: a new frontier in feedback. *IEEE Control Systems* 1997; **17**(6):19–35.
2. Housner GW, Bergman LA, Caughey TK, and others. Structural control: past, present, and future. *Journal of Engineering Mechanics*, ASCE 1997; **123**(9):897–971.
3. Kobori T *et al*. *Proceedings of the Second World Conference on Structural Control*, Kyoto, Japan. Wiley: New York.
4. Hsu CC, Calise AJ, Goodno BJ, Craig JI. Performance evaluation of robust controllers in earthquake structural dynamics problems. *Proceedings of the American Control Conference*, Seattle, Wa, 1995; 1916–1920.
5. Wan YK, Ghaboussi J, Venini P, Nikzad K. Control of structures using neural networks. *Smart Materials and Structures* 1995; **4**:49–57.
6. Skelton RE. Open problems in structural control. *Proceedings of ACC* 1995: 2339–2343.
7. Zhu G, Skelton RE. Output constraint problem with disturbance feedback. *Proceedings of the first World Conference on Structural Control*, Pasadena, CA, FP4, 1994; 32–41.
8. Spencer BF, Suhardjo J, Sain MK. Frequency Domain Optimal Control Strategies for Aseismic Protection. *Journal of Engineering Mechanics*, ASCE 1994; **120**(1):135–158.
9. Schmitendorf WE, Marti S, Jabbari F, Yang JN. Active control of seismically-excited buildings with model uncertainty. *Proceedings of Fifth U.S. National Conference on Earthquake Engineering*, Chicago, IL, 1994; 951–959.
10. Schmitendorf WE, Jabbari F, Yang JN. Robust control techniques for buildings under earthquake excitation. *Earthquake Engineering and Structural Dynamics* 1994; **23**:539–552.
11. Jannari F, Schmitendorf WE, Yang JN. $H_\infty$ Control for seismic-excited building with acceleration feedback. *Journal of Engineering Mechanics*, ASCE 1995; **121**(9):994–1002.
12. Kose IE, Schmitendorf WE, Jabbari F, Yang JN. $H_\infty$ Active seismic response control using static output feedback. *Journal of Engineering Mechanics*, ASCE 1996; **122**(7):651–659.
13. Yang JN, Wu JC, Agrawal AK. Sliding Mode Control of Seismic-Excited Linear Structures. *Journal of Engineering Mechanics*, ASCE 1995; **121**(12):1330–1339.
14. Yang JN, Wu JC, Agrawal AK. Sliding mode control of seismic-excited nonlinear and hysteretic structures. *Journal of Engineering Mechanics*, ASCE 1995; **121**(12):1386–1390.
15. Yang JN, Wu JC, Reinhorn AM, Riley M, Schmitendorf WE, Jabbari F. Experimental verification of $H_\infty$ and sliding mode control for seismically excited buildings. *Journal of Structural Engineering*, ASCE 1996; **122**(1):69–75.
16. Yang JN, Wu JC, Reinhorn AM, Riley M. Control of sliding-isolated buildings using sliding mode control. *Journal of Structural Engineering*, ASCE 1996; **122**(2):83–91.
17. Yang JN, Wu JC, Agrawal AK, Hsu SY. Sliding mode control with compensators for wind and seismic response control. *Earthquake Engineering and Structural Dynamics* 1997; **26**:1137–1156.
18. Agrawal AK, Yang JY. Optimal polynomial control of seismic-excited linear structures. *Journal of Engineering Mechanics*, ASCE 1996; **122**(7):753–761.
19. Agrawal AK, Yang JY. Static output polynomial control for linear structures. *Journal of Engineering Mechanics*, ASCE 1997; **123**(6):639–643.
20. Yang JN, Agrawal AK, Chen S. Optimal polynomial control of seismically excited nonlinear and hysteretic structures. *Earthquake Engineering and Structural Dynamics* 1996; **25**(11):1211–1230.
21. Cao H, Rienhorn AM, Soong TT. Design of an active mass damper for a tall TV tower in nanjing, China. *Journal of Engineering Structures* 1998; **20**(3):134–143.

 

22. Wu JC, Yang JN. Active control of a 310 meter TV transmission tower under stochastic wind. *Journal of Structural Engineering*, ASCE 1989; **124**(11):1302–1312.
23. Wu JC, Yang JN. Active control of Nanjing TV transmission tower with lateral-torsional motion. *Proceedings of the 5th SPIE, Smart Structures and Materials: Smart Systems for Bridges, Structures, and Highways*, vol. 3325, March 1–5, 1998, San Diego, CA, 1998; 22–34.
24. Spencer BF, Dyke SJ, Deoskar HS. Benchmark problems in structural control Part I: Active mass driver system; Part II: Active tendon systems. *Earthquake Engineering and Structural Dynamics* 1998; **27**:1127–1147.
25. Kose IE, Jabbari F, Schmitendorf WE, Yang JN. Quadratic stability and performance of a benchmark problem. *Earthquake Engineering and Structural Dynamics* 1998; **27**(11):1385–1397.
26. Wu JC, Yang JN, Agrawal AK. Applications of sliding mode control to benchmark problems. *Earthquake Engineering and Structural Dynamics* 1998; **27**:1247–1265.
27. Yang JN, Wu JC, Samali B, Agrawal AK. A benchmark problem for response control of wind-excited tall buildings. *Proceedings of the Second World Conference on Structural Control*, Kyoto, Japan, 1998; 1407–1416.
28. Spencer BF, Christermson RE, Dyke SJ. Next generation benchmark control problem for seismically excited buildings. *Proceedings of the Second World Conference on Structural Control*, Kyoto, Japan, 1989; 1351–1360.
29. Viellette RJ, Medanic JV, Perkins WR. Design of reliable control systems. *IEEE Transactions on Automatic Control* 1992; **37**(3):290–304.
30. Zhou K, Khargonekar PP, Stoustrup J, Niemann HH. Robust performance of systems with structured uncertainties in state space. *Automatica* 1995; **31**:249–255.
31. Boyd S. El Ghaoui L, Feron E, Balakrishnan V. *Linear Matrix Inequalities in System and Control Theory*. SIAM Publishing: Philadelphia, PA, 1994.
32. Gahinet P, Nemirovski Laub AJ, Chilali M. *LMI Control Toolbox*, The Mathworks Inc., 1995.
33. Alt TR. Robust control via quadratic Lyapunov functions with applications to reliability. *Ph.D. Dissertation*, Department of Mechanical and Aerospace Engineering, University of California, Irvine, 1997.
34. Kose IE, Jabbari F, Schmitendorf WE. A Direct Characterization of $L_2$ Gain Controllers for LPV systems. *IEEE Transactions on Automatic Control* 1998; **43**(9):1302–1306.
35. Jabbari F. Output feedback controllers for systems with structural uncertainty. *IEEE Transactions on Automatic Control* 1997; **42**(5):715–719, to appear.
36. Li Xi, deSouza CD. Delay dependent robust stability and stabilization of uncertain linear delay systems: a linear matrix inequality approach. *IEEE Transactions on Automatic Control* 1997; **42**:1144–1148.
37. Alt TR, Jabbari F. A reliable control system design for smart structures. ASME *International Congress*, San Francisco, CA, November 1995.
38. Alt TR, Jabbari F, Yang JN. Reliable control design for buildings under seismic excitation. *Eleventh World Conference on Earthquake Engineering* (11WCEE), Elsevier Science, Paper No. 1545, 1996.
39. Apkarian P, Gahinet P. A linear matrix inequality approach to $H_\infty$ control. *International Journal of Robust and Nonlinear* 1994; **4**:421–448.
40. Iwasaki T, Skelton R. All controllers for the general $H_\infty$ control problem: LMI existence condition and state space formulas. *Automatica* 1994; **30**(8):1307–1317.
41. Jabbari F, Kose IE. Design of controllers for disturbance attenuation of uncertain systems. ASME *Journal of Dynamics, Control and Measurement*, 1997 (Also in Proceedings of ASME International Congress, 1995).
42. Khargonekar PP, Petersen IR, Zhou K. Robust stabilization of uncertain linear systems: quadratic stabilization and $H_\infty$ control theory. *IEEE Transaction on Automatic Control* 1990; **35**:356–361.
43. Kose IE, Jabbari F. Disturbance attenuation for systems with real parametric uncertainty. *Proceedings of American Control Conference* (*ACC-97*), Albuquerque, New Mexico, 1997.
44. Schmitendorf WE, Jabbari F, Yang JN. An LMI approach for Robuster control laws for structures under environmental excitation. *Proceedings of IFAC*-96, San Francisco, 1996; 181–186.
45. Skelton RE, Stoustrup, Iwasaki T. The $H_\infty$ problem using static output feedback. *International Journal Robust and Nonlinear Control*. 1993; **4**:449–455

 